Quantum Hall Effects

João Carlos de Andrade Getelina
(Dated: November 23, 2018)

In this work we review the basic notions of quantum Hall effects. We present some of the theoretical approaches developed to investigate the integer and fractional quantum Hall effects (IQHE and FQHE, respectively). For the integer quantum Hall effect we focus on the determination of the quantized transverse conductance via gauge invariance arguments. Conversely, for the fractional quantum, we consider the variational method, which is based in introducing a trial wavefunction. We show that, in the thermodynamic limit, this trial wavefunction is related to a classical plasma in two dimensions, thus giving the relation for the quantization of the transverse conductance.

CONTENTS

I. INTRODUCTION

It is no longer a surprise that, in the microscopic level, the properties of a system become quantized. However, an experiment performed back in 1980 by von Klitzing *et al.* [1] showed a rather astonishing result: There are system which exhibit quantized macroscopic properties. This experiment consisted of a two-dimensional free electrons system under strong magnetic fields and low temperatures. It was observed a quite unusual behavior of the conductance with respect to the intensity of the magnetic field, consisting of relatively large steps of approximately constant conductance value. This phenomenon is now known as the quantum Hall effect (QHE), and it is believed to be one of the most important achievements of condensed matter physics in the past century.

Since its first discovery, much progress has been made in the area of QHE. There are now many known types of quantum Hall effects, but in particular we highlight the original ones, namely the integer quantum Hall effect (IQHE) and the fractional quantum Hall effect (FQHE). In the original paper by von Klitzing, it was observed the integer version. Only two years later, the FQHE was observed by Tsui et al. [2]. There are several important distinctions between these two effects, but the most basic one is that the conductance plateaus for the IQHE occur only at integer values of the ratio e^2/h, while for the FQHE these Hall conductance plateaus occur in rational values.

As one might guess, the QHE problem is a rather difficult one to solve: generally speaking, it involves a many-body interacting system in the presence of a disordered potential. Over the years much effort has been made in order to get a good theoretical description of the system. Even though we are still far from the ultimate microscopic theory, there are many theoretical approaches capable of encompassing various interesting physical properties. In a more technical sense, one of the major contributions of QHE was the establishment of a reliable standard for conductance/resistance. The reason is that the integer of rational values of the conductance plateaus are measured with a precision of about one part in 10^{10}, a rather remarkable figure.

The experimental observation of QHE has also paved the way to one of the most prolific areas in condensed matter physics nowadays, which is the topological phases of matter. The relation between topology and QHE is that the observed phases cannot be described by a local order parameter; these QHE phases present what is known as topological order. Furthermore, in a more speculative manner, there is also great interested around topological phases of matter directed to the application in quantum computing. Measurements of entanglement in those systems have shown no decoherence effects, a quite desirable feature for a quantum computer.

This remaining of this paper is organized as follows. In Sec. II we present the general experimental setup, and discuss some basic concepts needed to understand the quantum Hall problem, such as the Landau levels and the role of disorder. Sec. III is devoted to the IQHE, where we consider the gauge transformation approach [3, 4] in order to determine the quantized conductance analytically. The FQHE is presented and discussed in Sec. IV, where we give the general concepts of the variational method [5, 6]. Finally, in Sec. V we make an overview of the quantum Hall problem and we provide a discussion about what improvements are yet to be achieved.

II. BACKGROUND

In this section we introduce the basic concepts related to the quantum Hall effect. We start by introducing the general experimental setup, and we present the materials in which two-dimensional electron systems are realized. In addition, using classical electrodynamics theory, we compute the transverse conductance σ_{xy}, in order to compare to the experimental observations. Next, we investigate the Hamiltonian of a single carrier under an external magnetic field, and obtain the corresponding eigenvalues and eigenstates, which are known as the Landau levels. Finally, we discuss about the role of disorder in the quantum Hall effect, addressing the relation between random potentials and the existence of plateaus of conductance.

II.1. The experimental setup

The phenomenon dubbed as the Hall effect was discovered in the late XIX century, by Edwin Hall. He verified that carriers in a conductor sheet were deflected by the action of a magnetic field perpendicular to the system surface, thus originating a transverse potential difference V_{xy}. By measuring V_{xy} and applying Ohm's law, one can then determined the transverse resistance (or, equivalently, transverse conductance), which is known as the Hall resistance. Fig. 1 gives a schematic representation of this system.

It was only about a century later that the quantum Hall effect (QHE) was first observed [1]. The major difference between the quantum and classical versions of the Hall effect is the system in which they take place: while the latter occurs for any metal, the former was firstly observed in the surface of a semiconductor. Thus, the observation of the QHE coincides with a period in which semiconductors materials were intensively studied, mostly due to their

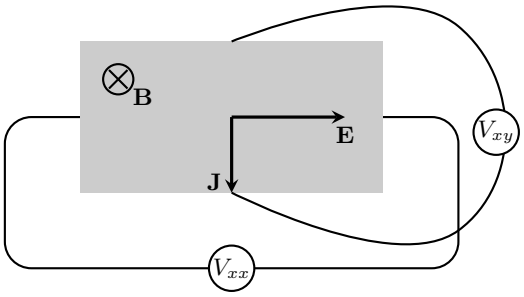

Figure 1. General experimental setup for Hall effects.

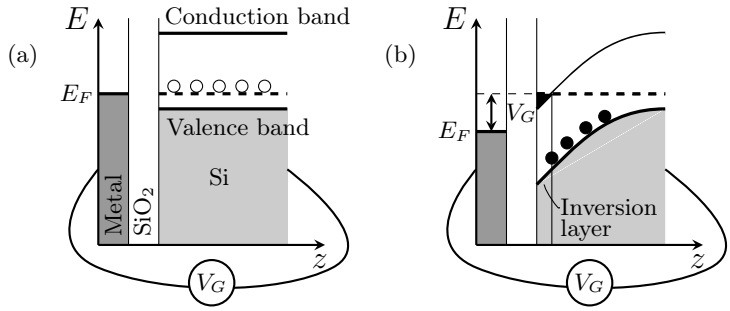

Figure 2. Schematic of a Si MOSFET for the cases (a) $V_G = 0$ and (b) $V_G > 0$. Adapted from Ref. [9].

technological applications. Another significant difference between the classical and quantum Hall effects is that the latter also requires stronger magnetic fields and much lower temperatures than the former.

The QHE was first observed in a Si MOSFET, i.e., a silicon metal-oxide-semiconductor field-effect transistor. In this system, a layer of SiO_2, which is an insulator, separates a layer of silicon doped with acceptors and a metal. There is also a potential difference V_G between the semiconductor and the metal, as shown in Fig. 2. The role of V_G is to induce an electric field between the surface of the metal and the semiconductor, such as in a capacitor. As we increase V_G, the corresponding electric field bends the energy levels of the semiconductor, up to the point where the conduction band gets below the Fermi level, as shown in Fig. 2. In this case, the electrons near the semiconductor surface are able to occupy the conduction band, thus being able to move freely in the xy plane. This thin layer close to the semiconductor surface is known as the inversion layer. Notice that the electron density of the inversion layer, which is usually set about 10^{15}–$10^{17}\mathrm{m}^{-2}$, can be controlled by the gate potential V_G.

An important property of the Si MOSFET to note is the existence of charged acceptors within or close to the inversion layer, as shown in Fig. 2. These atoms act as impurities, which generate a position-dependent random potential for the electrons in the conduction band. As we shall see, this random potential plays a major role in the understanding of the integer quantum Hall effect. There are systems in which the effect of the random potential can be better controlled, such as in GaAs-AlGaAs heterojuctions. In these systems, it has been observed both the integer [7] and fractional [2] Hall effects. For our purposes, it suffices to discuss the properties of the Si MOSFET; the reader interested in other heterojunctions may look at Refs. [8, 9]. In addition, it is important to emphasize that the QHE is not restricted to semiconductor heterojuctions; recently, for example, it has been verified QHE in graphene at room temperature [10].

Since we have already established the general experimental setup, as depicted in Fig. 1, we can now make predictions about the behavior of the transverse conductance σ_{xy}. For instance, according to classical electrodynamics, the steady-state solution is given by equating the forces due to the electric and magnetic fields, i.e.,

$$e\mathbf{E} = -e\mathbf{v} \times \mathbf{B}, \tag{1}$$

which gives us the following drift velocity:

$$v = -\frac{E}{B}. \tag{2}$$

Notice that the drift velocity is perpendicular to the electric field. Thus, the particle travels in equipotential lines. In

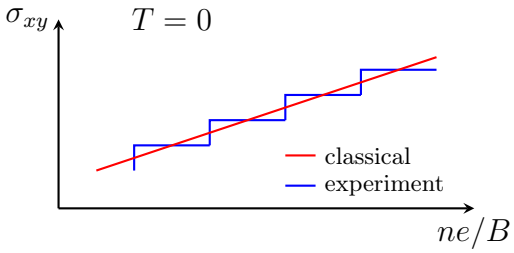

Figure 3. Sketch of the transverse conductance σ_{xy} accordingly to the classical prediction and the experimental observation, at zero temperature.

addition, the current density J is given by

$$J = -nev, \tag{3}$$

where n is the electron density. The connection between the current density and the electric field is given by the conductivity tensor $\boldsymbol{\sigma}$, i.e., $\mathbf{J} = \boldsymbol{\sigma}\mathbf{E}$. Thus, substituting the drift velocity in the previous equation, we find an expression for the transverse conductance σ_{xy}:

$$\sigma_{xy} = \frac{ne}{B}. \tag{4}$$

(Similarly, the longitudinal conductance is $\sigma_{xx} = 0$.) Hence, according to classical electrodynamics, the transverse conductance increases linearly with the ratio n/B.

However, under strong magnetic fields and low temperatures, the picture observed experimentally is quite different from the classical prediction, as illustrated in Fig. 3. As aforementioned, the experiment exhibits plateaus of transverse conductance, which are given by the following expression

$$\sigma_{xy} = \frac{e^2}{2\pi\hbar}\nu, \tag{5}$$

where $\nu \in \mathbb{N}$. The integer value ν, which is known as the filling factor, is measured with a rather astonishing precision: in the order of one part in 10^{10} for some filling factors close to the center of its plateau. Thanks to this precision, the Hall resistance $\rho_{xy} = 1/\sigma_{xy}$ became the standard value of resistance. Finally, the simple appearance of $\hbar$ in Eq. (5) tells us that we need a quantum treatment of the problem to obtain the correct behavior of the Hall conductance, as we address in the following.

II.2. Landau levels

Let us consider a single electron of charge $-e$, confined to the xy plane, under the presence of an external magnetic field $\mathbf{B} = -B\hat{z}$. The Hamiltonian of this system is given by

$$H_0 = \frac{1}{2m}\left(\mathbf{p} + e\mathbf{A}\right)^2 = \frac{1}{2m}\boldsymbol{\pi}^2. \tag{6}$$

The gauge choice in problems containing the vector field $\mathbf{A}$ is very important, since a wise choice may simplify the problem considerably. In QHE systems, there are two gauge choices that proved to be useful, namely the Landau gauge and the symmetric gauge. The Landau gauge is especially suited for problems in a rectangular geometry. It is given by the following relation:

$$\mathbf{A} = -xB\hat{y}. \tag{7}$$

On the other hand, the symmetric gauge is defined as

$$\mathbf{A} = \frac{B}{2}\left(y\hat{x} - x\hat{y}\right). \tag{8}$$

This gauge is useful for problems with rotational symmetry.

However, there is a faster way of obtaining the energy spectrum of (6) without referring to any gauge. First, notice that the commutator between the components of $\boldsymbol{\pi}$ is given by

$$[\pi_x, \pi_y] = -i\frac{\hbar^2}{l_0^2}, \tag{9}$$

where $l_0 = \sqrt{\hbar/eB}$ is the magnetic length. Therefore, by a proper normalization, the two components of $\boldsymbol{\pi}$ give a pair of canonical operators. Since the Hamiltonian is a sum of the squares of canonical operators, we may proceed as in the harmonic oscillator, where we introduce the dimensionless creation/annihilation operators:

$$a^\dagger = \frac{1}{\hbar\sqrt{2}}\left(\pi_x + i\pi_y\right), \qquad a = \frac{1}{\hbar\sqrt{2}}\left(\pi_x - i\pi_y\right), \tag{10}$$

Hence, the Hamiltonian is rewritten as

$$H_0 = \hbar\omega_c\left(a^\dagger a + \frac{1}{2}\right), \tag{11}$$

where $\omega_c = eB/m$ is the cyclotron frequency, and, consequently the eigenvalues are given by

$$E_n = \hbar\omega_c\left(n + \frac{1}{2}\right), \quad n = 0, 1, \ldots \tag{12}$$

The corresponding eigenstates are known as the Landau levels. Throughout this work we are going to be interested in calculating the system low-lying excitations. Thus, the lowest Landau level (LLL), i.e., the state with $n = 0$ will be constantly referred to.

The whole physics of the problem has not yet been captured. For instance, one would expect the electron to be described by two quantum numbers, since it is restricted to move in the xy plane. To find this extra quantum number, we will have to choose a gauge. As we shall see in the following, the second quantum number expresses the enormous degeneracy contained in each Landau level. To observe this huge degeneracy without explicitly determining the eigenstates, let us consider the following operator:

$$\mathbf{R} = X\hat{x} + Y\hat{x} = \mathbf{r} - \frac{l_0^2}{\hbar}\hat{z}\times\boldsymbol{\pi}. \tag{13}$$

The components of this operator also yield a canonical commutation relation, where $\hbar$ is replace by l_0^2. Thus, we may employ the Bohr-Sommerfeld quantization rule, in which the area of the phase space is proportional to h. Here, the area of the phase space corresponds to the area of the sample itself, which is given by L_xL_y. Therefore, the degeneracy D of each Landau level is given by

$$D = \frac{L_xL_y}{2\pi l_0^2} = \frac{L_xL_yeB}{2\pi\hbar} = \frac{1}{\Phi_0}L_xL_yB = \frac{\Phi}{\Phi_0}, \tag{14}$$

where $\Phi_0 = 2\pi\hbar/e$ is the flux quanta. This enormous degeneracy forbids us to employ perturbation theory in order to include the interactions and impurities in Hamiltonian.

Diving D by the number of particles N we get the number of available states per particle, i.e.,

$$\frac{D}{N} = \frac{L_xL_y}{N}\frac{eB}{2\pi\hbar} = \frac{eB}{2\pi n\hbar}. \tag{15}$$

Note that the right-hand side of the expression above is obtained if we equate Eqs. (4) and (5), which corresponds to the points where the classical prediction intercepts the experimental result. Thus, we get the following relation

$$\frac{D}{N} = \frac{1}{\nu}. \tag{16}$$

This expression is useful to interpret the fractional quantum Hall effect; for instance, the filling factor $\nu = 1/3$ tells us that there are three available states per particle at the LLL. On the other hand, for the integer quantum Hall effect, ν gives us the number of filled Landau levels.

To determine the eigenstates of (6) we will consider both the Landau and the symmetric gauge, Eqs. (7) and (8), respectively. As we shall verify in the next sections, the former is more adequate to the IQHE, while the latter is used to describe the FQHE. Let us consider first the Landau gauge. Substituting Eq. (7) in (6) we find

$$H_0 = \frac{1}{2m}\left[p_x^2 + (p_y - eBx)^2\right]. \tag{17}$$

Note that the expression above is translationally invariant in the y-direction. Thus, one may look for solutions as the following:

$$\psi_k(x,y) = f(x)\, e^{iky}. \tag{18}$$

Using this Ansatz, one may find that the Hamiltonian corresponds to a harmonic oscillator with the center displaced by $-kl_0^2$. Hence, the complete eigenfunctions (ignoring the normalization) are given by

$$\psi_{n,k}(x,y) = e^{iky} H_n(x)\, e^{-\left(x-kl_0^2\right)^2/2l_0^2}, \tag{19}$$

where $H_n(x)$ are the Hermite polynomials.

Conversely, by inserting the symmetric gauge (8) in (6) we find

$$H_0 = \frac{1}{2m}\left[\left(p_x + \frac{B}{2}y\right)^2 + \left(p_y - \frac{B}{2}x\right)^2\right]. \tag{20}$$

This Hamiltonian commutes with the z-component of the angular momentum, thus we may use the eigenvalue of L_z as a quantum number. In addition, notice that L_z may be written in terms of the two pairs of canonical operators, namely $\boldsymbol{\pi}$ and $\mathbf{R}$:

$$L_z = -\frac{\hbar}{2l_0^2}\left(X^2 + Y^2\right) + \frac{l_0^2}{2\hbar}\left(\pi_x^2 + \pi_y^2\right). \tag{21}$$

Hence, we can introduce new creation/annihilation operators, b and $b^\dagger$ respectively, which are related to $\mathbf{R}$, similarly to Eq. (10). Thus, we obtain

$$L_z = \hbar\left(a^\dagger a - b^\dagger b\right), \tag{22}$$

with a general eigenstate given by

$$|n,m\rangle = \frac{\left(a^\dagger\right)^n \left(b^\dagger\right)^m}{\sqrt{n!}\sqrt{m!}}\,|0,0\rangle. \tag{23}$$

Here, the quantum number n gives the energy, while m gives the degeneracy. To obtain the eigenstates (23) in the coordinate representation, it is convenient to introduce complex variables $z = x + iy$. For the lowest Landau level (LLL), we have the condition $a\,|LLL\rangle = 0$, which gives (ignoring the normalization)

$$\psi_{LLL}(z) = z^m e^{-|z|^2/4l_0^2}, \qquad m = 0, 1, 2, \ldots \tag{24}$$

This eigenfunction will be frequently used in the investigation of the FQHE.

Finally, notice that throughout this discussion, we have omitted the electric field. The reason is that the effect of the electric field is equivalent to what we observed in the classical case; the superposition of the cyclotron motion and a constant drift velocity perpendicular to the electric field. Moreover, as a side note, one could argue about the role of the electron spin, since the magnetic field lifts up the spin degeneracy. It is reasonable to assume that, under such strong magnetic fields, the spins are all polarized, i.e., pointing in the same direction of the magnetic field. In practice, however, the electron spin does indeed play a role, especially in the case of some exotic filling factors in the fractional quantum Hall effect. Nevertheless, for the sake of simplicity, we disregard the electron spin throughout this work.

II.3. The role of disorder

Before providing an explicit calculation of the transverse conductance, we make a phenomenological discussion about the existence of the Hall resistance plateaus, as depicted in Fig. 3. As we have discussed previously, the presence of impurities affecting the inversion layer is inevitable. However, according to Anderson localization theory [11], any amount of disorder in a two-dimensional system at zero temperature makes every state localized. Thus, the observation of a Hall current would be impossible, since transport only occurs for extended states in zero temperature. Nevertheless, the experiment shows that there is indeed a Hall current.

The explanation for this inconsistency between localization theory and the QHE experimental observation relies on the complete disregard of the Hall conductance in the development of the one-parameter scaling theory of localization.

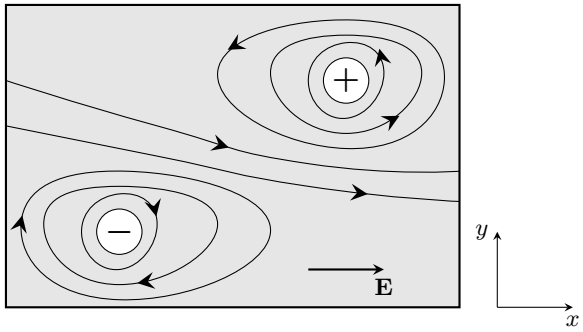

Figure 4. Bending of the equipotential lines caused by a random potential. Here, we are considering a region of the system away from the edges.

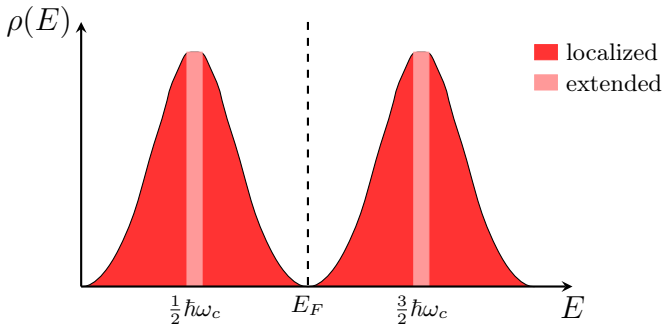

Figure 5. Density of states $\rho(E)$ of the electron in a magnetic field and in the presence of a random potential. E_F denotes the Fermi level. Adapted from Ref. [9].

However, there has been some efforts in order to include the Hall conductance, and hence the effect of magnetic fields, in the scaling theory of localization. First attempts considered a two-parameter scaling theory, which was able to predict the basic features of conductance, and also a shift in the position of the extended states in the energy spectrum as disorder becomes comparable to the Landau levels gap [12]. Further improvements were achieved by a three-parameter scaling theory, which included the electron-electron interactions. This theory was able to predict a order-disorder phase transition, corresponding to the destruction of the QHE [13].

To understand how disorder affects the properties of the system states, let us first consider the case free of randomness, in which the single-particle states are given by the Langau gauge eigenstates in (19). Notice that the these states are extended in the y-direction since they are described by a plane wave, and are thus able to contribute to the Hall current. Now let us turn on the random potential caused by impurities. Suppose that this random potential have some local maxima and minima, as depicted in Fig. 4. Thus, the equipotential lines generated by the applied electric field are no longer longitudinal; the extreme points of the random potential will bend the equipotential lines, making a closed trajectory around them (see Fig. 4). Therefore, an electron which falls into one of these enclosed potential lines becomes localized and thus cannot contribute to the Hall current.

One could argue, however, whether this localization mechanism induced by the random potential is able to localized all the system states. From the experimental point of view, one knows that this is not possible since the Hall current is indeed observed. On the other hand, as we shall see in the next section, from the theoretical point of view it is necessary to assume that at least one of the system states remains extended in the presence of disorder [4]. It was later verified from both numerical and analytical calculations that the system density of states in the presence of disorder is as follows: There is a small region of extended states near the eigenvalues of the Landau levels in the absence of disorder. This small region is surrounded by localized states only, as depicted in Fig. 5. Therefore, according to this picture, as we vary the Fermi level E_F, either by changing the electrons density or the magnetic field, the Hall conductance remains constant since localized states do not contribute to the current; we only observe a change in the transverse conductance as we reach the next extended state, which corresponds to the sharp steps in between the plateaus.

This configuration of the density of states, in which a small region of extended states is enclosed by localized ones, has been extensively verified via numerical methods. One can find delocalized states by observing the variation of the

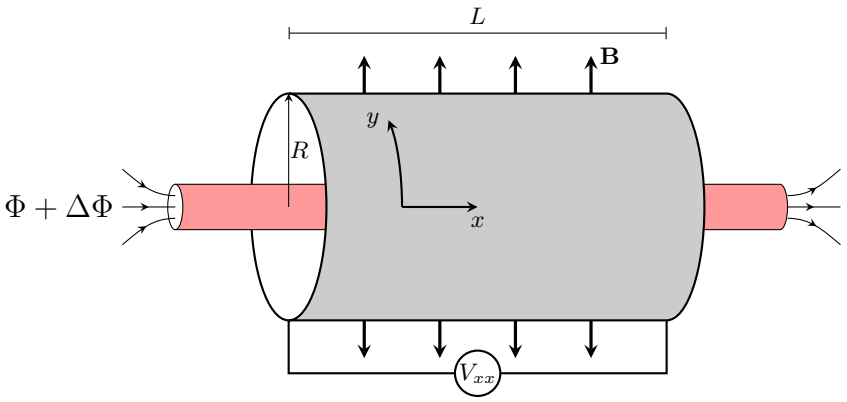

Figure 6. Transformed quantum Hall system as a cylinder of radius R and length L, with a flux Φ passing through the center. Adapted from Ref. [9].

localization length ξ with respect to the energy. Indeed, it has been observed that close to the Landau level energies, the localization length diverges as [14]

$$\xi \propto |E - E_c|^{-\nu}, \qquad \nu = 2.35 \pm 0.08,$$

where E_c is the corresponding Landau level energy. This exponent has not yet been determined analytically.

III. INTEGER QUANTUM HALL EFFECT

To explain the conductance plateaus in the IQHE, Laughlin came up with a rather elegant argument, based solely in properties of gauge invariance. Consider our QHE system on the surface of a cylinder of radius R and length L, as shown in Fig. 6. The y-direction surrounds the system surface while the x-direction is parallel to the cylinder axis. Thus, the magnetic field $\mathbf{B}$ must be radial with respect to the cylinder axis. Even though this configuration is not useful for experimental purposes, since the periodic boundary condition in the y-direction does not allow for measurements of the Hall conductance, it provides us a fast calculation of the quantization of σ_{xy}.

The key point to argument is to add a solenoid in the center of the cylinder, as depicted in Fig. 6. This solenoid generates a magnetic flux Φ, and, according to the Aharonov-Bohm effect, this flux induces a vector potential $\mathbf{A}_\Phi$ on the system. From Stoke´s law, one may find that

$$\Phi = \oint d\mathbf{l} \cdot \mathbf{A}_\Phi = 2\pi R \left|\mathbf{A}_\Phi\right|. \tag{25}$$

This change in the vector potential may be thought of as a gauge transformation.

Consider now a flux variation $\Delta\Phi$ in the solenoid. This induces a phase shift in the electron wavefunction, which is given by

$$\psi(x,y) \to \psi(x,y)\, e^{-iey\Delta\Phi/(hR)}. \tag{26}$$

However, in the configuration we considered, the boundary conditions do not allow any gauge transformation to take place. We have to consider two possibilities: (i) the states in the surface are extended or (ii) the states in the surface are localized. For the latter case, any continuous gauge transformation is permitted. Conversely, for the case (i), the gauge transformation must respect a full phase shift, i.e, $\psi(x, y + 2\pi R) = \psi(x,y)$, implying that

$$\Delta\Phi = \frac{h}{e} \times \text{integer}. \tag{27}$$

Therefore, to obtain any relevant change to the system wavefunctions, we have to assume that the states are extended. We then look to the situation in which the flux variation does not respect the criterion (27). In this case, since the total vector potential is given by

$$\mathbf{A} + \mathbf{A}_\Phi = B\left(x - \frac{\Phi}{2\pi RB}\right)\hat{y}, \tag{28}$$

a flux variation $\Phi \to \Phi + \Delta\Phi$ will only cause a shift in the x-direction. Hence, the electron extended states simply move to the next one along the cylinder axis. Under the presence of disorder, some of the extended states will be transformed into localized ones. The latter are not able to move along the x-direction, regardless whether (27) is satisfied. On the other hand, the remaining extended states are still able to pass through these localized ones. Thus, it suffices to postulate that there is at least one extended state in the random system.

Now recall that in the IQHE, all extended states below the Fermi level are occupied. Thus, if we consider a flux variation $\Delta\Phi = h/e$, all electrons must move to the next extended states. However, at the end of the cylinder, the electron in the last extended state flows out of the system, which is then supplied with another electron by the electrode. Hence, the number of electrons ν that flows in/out of the system corresponds to the number of Landau levels below the Fermi level. The energy cost of this process is given by

$$\Delta E = eV_{xx}N. \tag{29}$$

We can relate this energy cost to the current density in the y-direction as follows:

$$\begin{aligned} J_y &= -\frac{1}{2\pi RL}\left\langle \sum_i \frac{e}{m}\left[p_{iy} + eA_y\left(r_i\right)\right]\right\rangle \\ &= \frac{1}{L}\left\langle \frac{\partial}{\partial\Phi}\left\{\sum_i \frac{1}{2m}\left[p_{ix}^2 + \left(p_{iy} + eA_y\right)^2\right] + V_{\text{imp}}\left(r_i\right)\right\}\right\rangle \\ &= \frac{1}{L}\left\langle \frac{\partial H}{\partial\Phi}\right\rangle = \frac{1}{L}\frac{\partial}{\partial\Phi}\left\langle E\right\rangle. \end{aligned} \tag{30}$$

Therefore, the transverse current density is proportional to the variation in the system energy with respect to the variation of the solenoid flux. Finally, we obtain

$$J_y = \nu\frac{e^2}{2\pi\hbar}\frac{V_{xx}}{L} = \nu\frac{e^2}{2\pi\hbar}E_x, \tag{31}$$

which gives the transverse conductance

$$\sigma_{xy} = -\nu\frac{e^2}{2\pi\hbar} \tag{32}$$

as expected.

Even though the gauge arguments provided by Laughlin and Halperin are able to capture the quantization of the Hall conductance, it still lacks a microscopic description of IQHE systems. The best approach so far in the direction towards the ultimate microscopic theory of the IQHE was developed by Pruisken [12, 15]. Based on the σ-model for disordered electron systems, Pruisken was able to derive an action which includes the effects of magnetic fields. Using this action, it is possible to describe much of the physics of IQHE. In addition, this theory allows one to use renormalization group methods.

IV. FRACTIONAL QUANTUM HALL EFFECT

The first observation of a fractional filling factor, namely $\nu = 1/3$, happened just two years after the observation of the IQHE [2]. In succession to this discovery was the observation of the filling factor $\nu = 2/3$ [16]. These observations were quite surprising at the time, as the theory of the IQHE was already on course, and the mechanism of localization due to disorder suggested that only integer filling factors were possible. The missing ingredient of the IQHE theories was the electron-electron interactions. After those two pioneering works on the FQHE, many other observations of fractional filling factors were made. Nowadays, there are about 80 different known filling factors. However, this experimental progress has not been matched by the theory; there are many filling factors still lacking a theoretical explanation.

The major difference between the integer and fractional QHE effects in the inclusion of electron-electron interactions in the latter. Hence, for the FQHE we can write down the Hamiltonian as

$$H = \frac{1}{2m}\sum_i\left[\boldsymbol{\pi}_i^2 + V_{\text{imp}}\left(\mathbf{r}_i\right)\right] + \frac{1}{2}\sum_{i\neq j} V\left(\left|\mathbf{r}_i - \mathbf{r}_j\right|\right), \tag{33}$$

where $V_{\text{imp}}(\mathbf{r})$ is the random potential caused by the impurities, and $V(|\mathbf{r}_i - \mathbf{r}_j|)$ stands for the electron-electron interactions. The usual approach to face a problem such as in Eq. (33) is to assume the interaction term as a small perturbation to the remaining terms, and employ perturbation theory. However, as we have discussed previously, the massive degeneracy of the Landau levels forbids us to even start a perturbative method.

The first alternative to the perturbative approach was developed by Laughlin [5]. The author had a great deal of physical insight of the problem, where he imagined that electrons in FQHE systems would like to stay as far from each other as possible. Hence, inspired by previous works on liquid helium, a system where the particles also prefer to be far apart from each other, he proposed a trial wavefunction, which is the following:

$$\psi(z_i) = \prod_{i<j} (z_i - z_j)^m \exp\left(-\sum_{k=1}^{N} \frac{|z_k|^2}{4l_B^2}\right), \tag{34}$$

where m is an odd integer, in order to respect Pauli's principle.

Given this trial wavefunction, let us consider the expectation value of a general operator $\mathcal{O}(z)$. Hence, From the definition, we have

$$\langle \mathcal{O}(z) \rangle = \frac{\int \prod_i d^2 z_i \mathcal{O}(z) P[z_i]}{\int \prod_i d^2 z_i P[z_i]}, \tag{35}$$

where the unnormalized probability distribution $P[z_i]$ is defined as

$$P[z_i] = \prod_{i<j} \frac{|z_i - z_j|^{2m}}{l_B^{2m}} \exp\left(-\sum_{k=1}^{N} \frac{|z_k|^2}{4l_B^2}\right). \tag{36}$$

The expectation value in (35) is very difficult to compute. However, notice that by writing $P[z_i] = e^{-\beta H(z_i)}$, and setting $\beta = 2/m$, we find:

$$H(z_i) = \frac{1}{2\beta l_B^2} \sum_i |z_i|^2 - \frac{2m}{\beta} \sum_{i<j} \ln\left(\frac{|z_i - z_j|}{l_B}\right). \tag{37}$$

The expression above corresponds to the energy of a classical one-component plasma of charged particles in two-dimensions. For instance, consider that this plasma is composed of particles with charge $-\sigma$, and a background potential density ρ. Hence, the corresponding potential energy is given by

$$U(z_i) = \frac{\rho\sigma}{4\epsilon} \sum_i |z_i|^2 - \frac{\sigma^2}{2\pi\epsilon} \sum_{i<j} \ln\left(\frac{|z_i - z_j|}{l_B}\right), \tag{38}$$

where ϵ is the dielectric constant. Thus, in the thermodynamic equilibrium, the particle density of the plasma is $n = \rho/\sigma$.

By comparing Eqs. (37) and (38), we find that

$$\frac{\rho\sigma}{4\epsilon} = \frac{1}{2\beta l_0^2}, \qquad \frac{\sigma^2}{2\pi\epsilon} = \frac{2m}{\beta}, \tag{39}$$

which gives

$$\frac{1}{m} = 2\pi l_0^2 n. \tag{40}$$

Finally, according to Eqs. (15) and (16), we find that

$$\nu = \frac{1}{m}. \tag{41}$$

Thus, in the thermodynamic limit, the Laughlin wavefunction (34) represents a state with filling factor $1/m$. For completeness, in Table I we show the overlap between the Laughlin wavefunction and the exact diagonalization result for a few particles. Notice that there is a quite good agreement.

N	Matrix dimension	$\langle\psi_0\vert\ \psi_{\text{exact}}\rangle$
4	15	0.99804
5	73	0.99906
6	338	0.99644
7	1656	0.99636
8	8512	0.99540
9	45207	0.99406

Table I. Overlap between the Laughlin wavefunction and the exact ground state obtained numerically for the filling factor $\nu = 1/3$. Adapted from Ref. [17].

V. CONCLUDING REMARKS

In this work we have reviewed one of the most relevant discoveries of the past century in the area of condensed matter physics, which is the quantum Hall effect. We have provided a general background for the problem while discussing the experimental setup, the single-particle eigenstates and the role of disorder. For the integer filling factors case, we have limited our discussion to the calculation of the transverse conductance from the gauge invariance arguments. Other important approaches have been neglected, such as those concerning the existence of edge states, and the field-theoretical approach [12, 15]. Conversely, for the fractional filling factor case, we considered the trial wavefunction developed by Laughlin, and compared the overlap between this theory and exact numerical calculations, which shows a good agreement for few electrons.

It is clear that the quantum Hall effect is still an open problem. For instance, in the case of the FQHE, the theoretical approaches developed so far are not able to capture the physics of any observed filling factor. In addition, it has not yet been determined the critical filling factor upon which the Wigner crystal phase becomes energetically more favorable. Other important discrepancy between theory and experiment relies on the measurement of the energy gap. States which are not incompressible fluids, such as the ones with even-denominator filling factor, are still not completely understood. Finally, as a guidance for further investigations, one could argue the investigation of strong magnetic field effects in lower-dimensional systems, such as one-dimensional chains or quantum dots.

[1] K. v. Klitzing, G. Dorda, and M. Pepper, Phys. Rev. Lett. **45**, 494 (1980).
[2] D. C. Tsui, H. L. Stormer, and A. C. Gossard, Phys. Rev. Lett. **48**, 1559 (1982).
[3] R. B. Laughlin, Phys. Rev. B **23**, 5632 (1981).
[4] B. I. Halperin, Phys. Rev. B **25**, 2185 (1982).
[5] R. B. Laughlin, Phys. Rev. Lett. **50**, 1395 (1983).
[6] R. B. Laughlin, Phys. Rev. B **27**, 3383 (1983).
[7] M. A. Paalanen, D. C. Tsui, and A. C. Gossard, Phys. Rev. B **25**, 5566 (1982).
[8] R. E. Prange and S. M. Girvin, eds., *The Quantum Hall Effect* (Springer New York, 1990).
[9] D. Yoshioka, *The Quantum Hall Effect* (Springer Berlin Heidelberg, 2002).
[10] K. S. Novoselov, Z. Jiang, Y. Zhang, S. V. Morozov, H. L. Stormer, U. Zeitler, J. C. Maan, G. S. Boebinger, P. Kim, and A. K. Geim, Science **315**, 1379 (2007), http://science.sciencemag.org/content/315/5817/1379.full.pdf.
[11] E. Abrahams, P. W. Anderson, D. C. Licciardello, and T. V. Ramakrishnan, Phys. Rev. Lett. **42**, 673 (1979).
[12] A. M. M. Pruisken, Phys. Rev. B **32**, 2636 (1985).
[13] R. B. Laughlin, M. L. Cohen, J. M. Kosterlitz, H. Levine, S. B. Libby, and A. M. M. Pruisken, Phys. Rev. B **32**, 1311 (1985).
[14] B. Huckestein, Rev. Mod. Phys. **67**, 357 (1995).
[15] A. Pruisken, Nuclear Physics B **235**, 277 (1984).
[16] H. Stormer, D. Tsui, A. Gossard, and J. Hwang, Physica B+C **117-118**, 688 (1983).
[17] G. Fano, F. Ortolani, and E. Colombo, Phys. Rev. B **34**, 2670 (1986).